Rapid malachite green removal from aqueous solution by natural zeolite: process optimization by response surface methodology

Mehtap Tanyol

Department of Environmental Engineering, Munzur University, Tunceli, Turkey, Tel. +90 428 2131794; Fax: +90 428 2131861; email: mtanyol@munzur.edu.tr

ABSTRACT

In this study, malachite green removal from aqueous solutions by natural zeolite was investigated. The interaction between zeolite and malachite green was determined by SEM/EDX and FTIR. The parameters like adsorbent dosage (0.1–1 mg/100 mL), initial malachite green concentration (40–200 mg/L) and the contact time (10–600 s) were optimized using the central composite design of response surface methodology. Maximum removal yield (99.70%) was obtained at an adsorbent dosage of 0.68 mg/100 mL, an initial malachite green concentration of 79.02 mg/L, and at 414 s contact time. The equilibrium process complied better with the Langmuir isotherm model, which exhibits a single layer adsorption, when compared with the Freundlich isotherm model. Adsorption kinetics followed the pseudo-second-order type kinetic and intra-particle diffusion played an important role onto adsorption mechanism of malachite green. The findings of this study demonstrated that zeolite which is found abundant on earth as a cheap and efficient adsorbent could be used for rapid malachite green adsorption from aqueous solutions.

Keywords: Malachite green; Natural zeolite; Response surface methodology; Isotherm; Kinetic

1. Introduction

Synthetic dyes are widely used in several industries particularly for textile, tannery, paper, plastics, pharmaceutical, and food industries. Commercial paint has more than 100,000 types and every year more than 7×10^5 tones of coloring agents are manufactured [1].

Malachite green (MG), a cationic dye, is a common dye from the triphenylmethane dye category and is used widely for staining cotton, jute, paper, silk, wool, and leather [2]. In addition, MG is commonly used in aquaculture cultivation for fungus and parasitic treatment due to its high efficiency [3]. Despite its extensive use and consumption, MG could penetrate into food chain and might cause possible damage in humans and other terrestrial or aquatic living organisms through direct contact, respiration or digestion, as a result of its mutagenic, carcinogenic and teratogenic characteristics [2]. In addition to this characteristic, discharge of MG to hydrosphere might cause environmental degradation, since it gives an undesired color to water and reduces the

daylight penetration [4]. Hence, wastewater with MG content should be treated before being discharged to aquatic environments.

Several methods such as electrocoagulation, flotation, chemical oxidation, filtration, ion exchange, ozonation, membrane separation, microbial degradation and adsorption are developed for removal of dye from water [5]. Among these methods adsorption has higher efficiency due to its operation simplicity, capacity and adequacy for large quantities of dye removal and various inexpensive and nontoxic materials could be used as an adsorbent [6]. Besides, adsorption could be considered as an attractive and efficient method when the dyes are typically considered as stable against light and durable against oxidation and biodegradation [7]. In order to remove MG from wastewater use of several materials such as dead biomass [8], immobilized biomass [9], clay [10], active carbon [11], agricultural waste [12], agro-industrial waste [13], polymer [14], nanoparticle [15], carbon nanotube [16] is reported.

In this study, zeolite, which is one of the most abundant materials on earth and a geologically natural material that can be obtained inexpensively, is used as the adsorbent. Lattice structure of this material provides extensive interior and exterior surface area for ion exchange and chemical reactions. These pores act as a molecular sieve. Zeolites are naturally anions and they have capacity for high ion exchange [17]. MG removal from aqueous solutions via the use of zeolite is verified by former adsorption studies. In the study conducted by Han et al. [18], maximum MG removal capacity (q_{max}) is found as 27.34 mg/g through the use of Chinese natural zeolite and no optimization study was conducted.

In the optimization of adsorption studies by classical method, an independent parameter is altered while other parameters are kept at a constant level. Thus, the procedure becomes extremely time consuming and high-priced. Furthermore, the significant disadvantage is not being able to determine the effects of interaction between the parameters that are studied. In order to overcome this problem, analytical procedures are optimized using multivariate statistical techniques. Response surface methodology (RSM) is a common technical, statistical and mathematical program used for the optimization of multi variants. RSM facilitates to determine distinctive and interactive effects of parameters and process parameters could be optimized through limited number of experiments [19].

The aim of this study is to determine the optimum conditions for MG adsorption via zeolite through the use of RSM. In the adsorption process, initial MG concentration, adsorbent dosage and the effect of contact time were investigated through Central Composite Design (CCD). Furthermore, kinetics and isotherms of adsorption were studied. The adsorbent is characterized through the use of FTIR and SEM/EDX analyses.

2. Materials and methods

2.1. Adsorbate and adsorbent

The dye, MG oxalate, (C.I. Basic Green 4, C.I. Classification Number 42,000, chemical formula = $C_{52}H_{54}N_4O_{12}$, molecular weight = 927.00 g/mol) was obtained from Merck (Germany). Stock solution of MG (500 mg/L) was prepared by dissolving 500 mg MG in 1,000 mL distilled water.

Natural zeolite was obtained from a local company (Enli Mining) in Turkey. Chemical composition of the zeolite was analyzed by X-ray fluorescence spectrometry and was found as follows (in mass, %): SiO_2 68.62, Al_2O_3 12.64, FeO_3 1.50, MgO 0.84, CaO 1.89, Na_2O 0.70, K_2O 3.43, CuO 0.75, LOI 9.63. Granulated zeolite was grinded and sifted through a 60 mesh sieve. In order to remove the fine dust, zeolite samples were washed with distilled water, dried at 105°C for 15 h and kept sealed in a flask to be used later in adsorption studies.

2.2. Batch adsorption studies

Batch adsorption analysis for removal of MG was conducted in 250 mL Erlenmeyer flasks. 0.1–1 g of zeolite was added to 100 mL MG solution with different initial dye concentrations between 40 and 200 mg/L. The pH value of the solution was kept unchanged (measured pH value of 4.5). The solution mixture was shaken at room temperature (25°C)

in a shaker at 200 rpm and Erlenmeyer flask samples were retrieved at time intervals determined according to RSM design (between 10 and 600 s). The sorbent was separated from the solution by centrifuging for 5 min at 5,000 rpm. MG concentration in the remaining solution was analyzed at 615 nm using a UV spectrophotometer (UV-1800, Shimadzu). The removal efficiency of MG was calculated as:

$$\text{MG removal,} \% = 100 \times \frac{(C_0 - C_t)}{C_t} \tag{1}$$

where C_0 and C_t are the MG concentrations at $t = 0$ and $t = t$, respectively (mg/L).

Adsorbed dosage of MG was calculated via the following formula:

$$q = \frac{(C_0 - C_t) * V}{X} \tag{2}$$

where q is the adsorbed MG dosage (mg/g), V is the volume of the solution (L) and X is the mass of MG (g).

Kinetics and isotherm studies were conducted by using optimum adsorbent dosage determined via RSM at initial MG concentrations that vary between 40 and 160 mg/L. Batch adsorption experiments were conducted as explained above. Pseudo-first-order, pseudo-second-order and intra-particle diffusion models were tested for the kinetics study and Langmuir and Freundlich isotherm models were tested for the equilibrium study.

Regeneration studies have been performed in optimum conditions established in by the RSM. MG loaded zeolite was regenerated using 0.1 M NaOH. To desorb dye, adsorbent treated with dye was extracted with 0.1 M NaOH and then washed with distilled water until the wash solution reached to the natural pH. The adsorbent was dried for 24 h at 80°C for the next cycle. Regeneration experiments were repeated until the fifth cycle.

2.3. Experimental design

CCD was used to investigate the effects of contact time (10–600 s), adsorbent dosage (0.1–1 mg/100 mL) and initial MG concentration (40–200 mg/L) for removal of MG from aqueous solutions. 2^3 factorial, CCD was conducted for these three independent variables in five levels ($-\alpha$, -1, 0, 1, $+\alpha$) with 20 experiments composed of eight factorial points, six axial points and six center points. Range and levels are presented in Table 1. Design Expert Version 9 (Stat-Ease, USA)

Table 1
Level of independent variables in experimental design with CCD

Factors	Range and levels				
	$-\alpha$ (−1.682)	−1	0	+1	$+\alpha$ (+1.682)
X_1: Adsorbent dosage (g/100 mL)	0.1	0.282	0.55	0.817	1
X_2: Initial MG concentration (mg/L)	40	72.431	120	167.568	200
X_3: Contact time (s)	10	129.59	305	480.408	600

was used to optimize the levels of the independent variables and to evaluate the interaction of process variables. Percentage of MG removal is taken as a dependent output response variable. In addition, Design Expert Software was used for the statistical analysis, variance analysis (ANOVA) and graphical analysis of the findings. The mathematical relationship between the three independent variables could be written down with the following quadratic model [20,21]:

$$y = b_0 + \sum_{i=1}^{n} b_i x_i + \sum_{i=1}^{n} b_{ii} x_i^2 + \sum_{i=1}^{n-1} \sum_{j=i+1}^{n} b_{ij} x_i x_j \tag{3}$$

where y is the assumed response (percentage of MG removal), x_i and x_j are the independent variables, b_0 is the model constant, b_i is the linear coefficient, b_{ii} is the quadratic coefficient and b_{ij} the cross-product coefficient. Optimum values of the independent variables that provide the maximum removal are found by using the desirability function of Design Expert Software.

2.4. Characterization

Infrared analysis of zeolite samples was carried out with a FTIR Spectrometer (Thermo Nicoleti S10), between 400 and 4,000 cm⁻¹, before and after the adsorption. In order to obtain information about the surface morphologies of zeolite and MG loaded zeolite, scanning electron microscopy (SEM) was performed in Leo, Evo 40 SEM at accelerating voltage of 20 kV attached to an X-ray energy dispersive spectrometer.

3. Results and discussion

3.1. Data analysis by response surface methodology

The effect of process variables, namely the initial MG concentration, adsorbent dosage and contact time, on the MG removal is investigated using CCD. Table 2 presents the coded values of the factors and design and the actual and predicted values of experimental results.

According to the experimental results, the empirical relationship with the response and independent variables is:

$$\begin{aligned} \text{Removal (\%)}, y &= 95.45 + 16.65\,X_1 - 6.95\,X_2 + 5.09\,X_3 \\ &\quad + 6.72\,X_1 X_2 - 2.42\,X_1 X_3 + 0.22\,X_2 X_3 \\ &\quad - 9.99\,X_1^2 - 0.51\,X_2^2 - 2.72\,X_3^2 \end{aligned} \tag{4}$$

While the positive sign in Eq. (4) shows the synergic effect, the negative sign indicates the antagonistic effect [22]. As observed in Eq. (4), the adsorbent dosage (X_1) and contact time (X_3) are positive, the initial MG concentration (X_2) is negative. These findings point out that MG adsorption could be developed further as the increase of adsorbent dosage and contact time. The results of ANOVA (Table 3) support the factual relationship between the proposed regression equation and important variables and reasonable response [22,23]. Additionally, the importance of the effect of three independent variables was evaluated using F-value and P-value with ANOVA results for the quadratic model. In this study, F-value was determined as 19.69 and P-value is smaller than the 0.0001 value, which verifies that the model

Table 2
Experimental design and results of CCD

Run	Factor 1 adsorbent dosage (X_1), g/100 mL	Factor 2 initial concentration (X_2), mg/L	Factor 3 contact time (X_3), (s)	MG removal, (%) Actual value	Predicted value
1	+1	+1	−1	94.49	95.75
2	0	0	0	95.71	95.45
3	+1.682	0	0	99.55	98.19
4	−1	+1	+1	92.22	91.53
5	+1	+1	+1	98.43	98.53
6	0	0	0	95.76	95.45
7	0	0	0	96.32	95.45
8	0	−1.682	0	99.58	99.69
9	0	0	0	95.15	95.45
10	0	+1.682	0	82.13	82.31
11	−1	+1	+1	61.35	59.64
12	−1.682	0	0	28.55	30.18
13	0	0	−1.682	72.10	71.19
14	−1	−1	+1	79.48	79.95
15	0	0	0	95.91	95.45
16	+1	−1	−1	99.37	99.66
17	+1	−1	+1	99.46	99.55
18	+1	+1	−1	50.68	54.16
19	0	0	+1.682	97.12	96.31
20	0	0	0	95.92	95.45

Table 3
ANOVA for response surface quadratic model

Source	Sum of squares	Df	Mean square	F-value	P-value prob > F
Model	6,698.09	9	744.23	19.60	< 0.0001
X_1-adsorbent dosage	3,787.22	1	3,787.22	99.73	< 0.0001
X_2-MG concentration	660.00	1	660.00	17.38	0.0019
X_3-contact time	353.83	1	353.83	9.32	0.0122
$X_1 X_2$	361.08	1	361.08	9.51	0.0116
$X_1 X_3$	46.95	1	46.95	1.24	0.2922
$X_2 X_3$	0.40	1	0.40	0.011	0.9199
X_1^2	1,439.11	1	1,439.11	37.90	0.0001
X_2^2	3.78	1	3.78	0.100	0.7587
X_3^2	106.80	1	106.80	2.81	0.1245

$R^2 = 0.95$, Adj $R^2 = 0.90$.
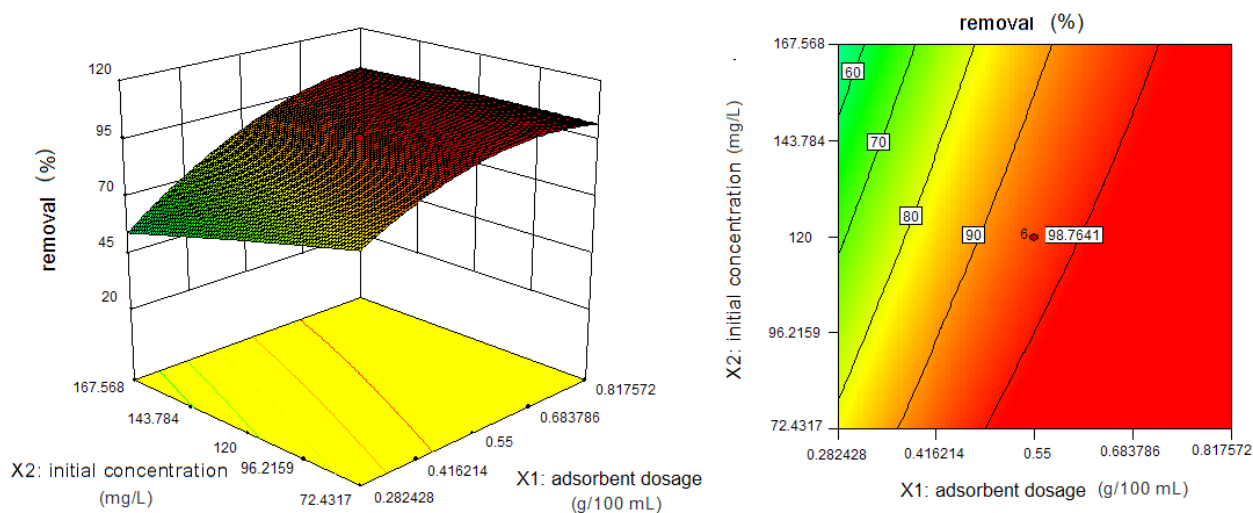
Fig. 1. The effect of adsorbent dosage and initial MG concentration on removal capacity, when the contact time was fixed to 305 s.

is statistically significant. As presented in Table 3, X_1, X_2, X_3, $X_1 X_2$ and X_1^2 are important model terms (P-value<0.05).

R^2, with a value of 0.95, indicates the convenience of the model for MG removal. R^2 value provides the measure of variability observed in response values, which could be explained by the experimental parameters and their inter-actions. R^2 value close to 1 estimates a better correlation between the predicted values and a better model response [24]. When R^2 value is stated in percentages, it means that 95% of the total variation for MG removal is ascribed to the independent variables and only 5% of the total variation could not be explained with the model. The adjusted R^2 (Adj R^2) value of the model is 0.90. Adj R^2 designates the R^2 value for the sample size and the number of variables in the model. As the model and sample size include multiple variables Adj R^2 could be smaller than the R^2 value.

Figs. 1–3 present the 3D response surface and contour plots, which indicate the effect of interaction between two independent variables related to the removal efficiency. In Fig. 1, it is possible to observe the effect of interaction between the adsorbent dosage (X_1) and the initial MG con-centration (X_2) on the removal efficiency, when the contact time is kept stable at 305 s. As the adsorbent dosage increased the removal efficiency increased, and the increase in concen-tration reduced the removal efficiency. This expected obser-vation actually is a result of the increasing adsorption due to the increase in initial dye concentration with respect to the increasing mass transfer from the concentration gradient, hence the concentration effect would have an inverse effect on the adsorption frequency, which shows the adsorption constant, since the adsorption surface for dye accumulation is limited for the adsorption frequency [25]. Sales et al. [26] also reported that an increase in the quantity of adsorbent material is possible to bring a higher percentage removal due to the increase in available surface area and exposure of the adsorption sites necessary for the removal of the dye. Similarly, in Fig. 2 it is possible to observe the effect of inter-action between the adsorbent dosage (X_1) and the contact time (X_3) on the removal efficiency, when the initial concen-tration is kept constant at 120 mg/L. Increasing contact time and adsorbent dosage until the maximum removal elevated the removal efficiency. Rapid MG adsorption is dependent on the vast number of pores and their structures in the adsorbent, which facilitates rapid penetration for MG at
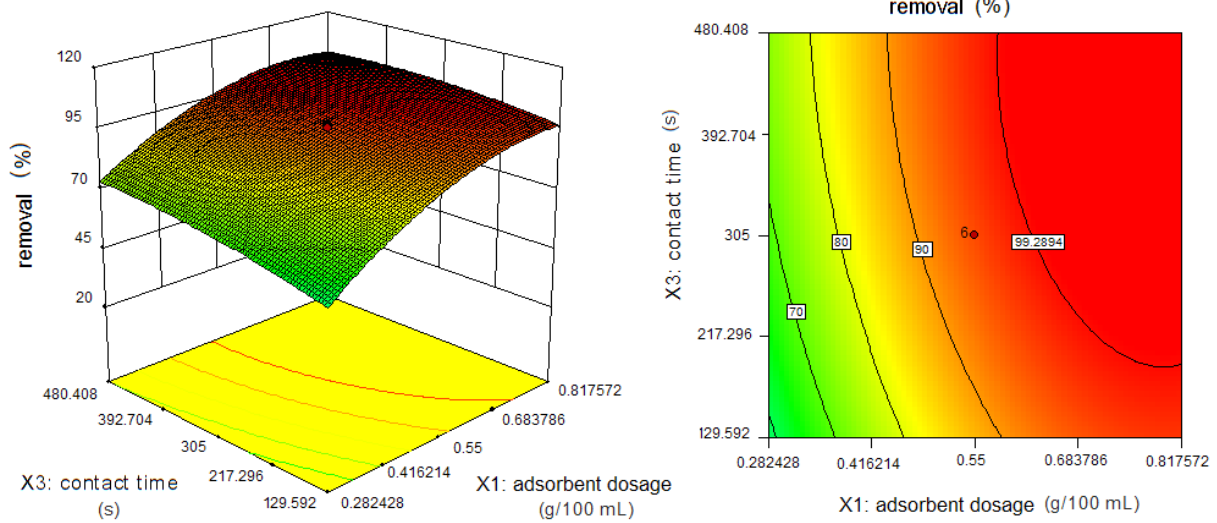
Fig. 2. The effect of adsorbent dosage and contact time on the removal capacity, when the initial MG concentration was fixed to 120 mg/L.
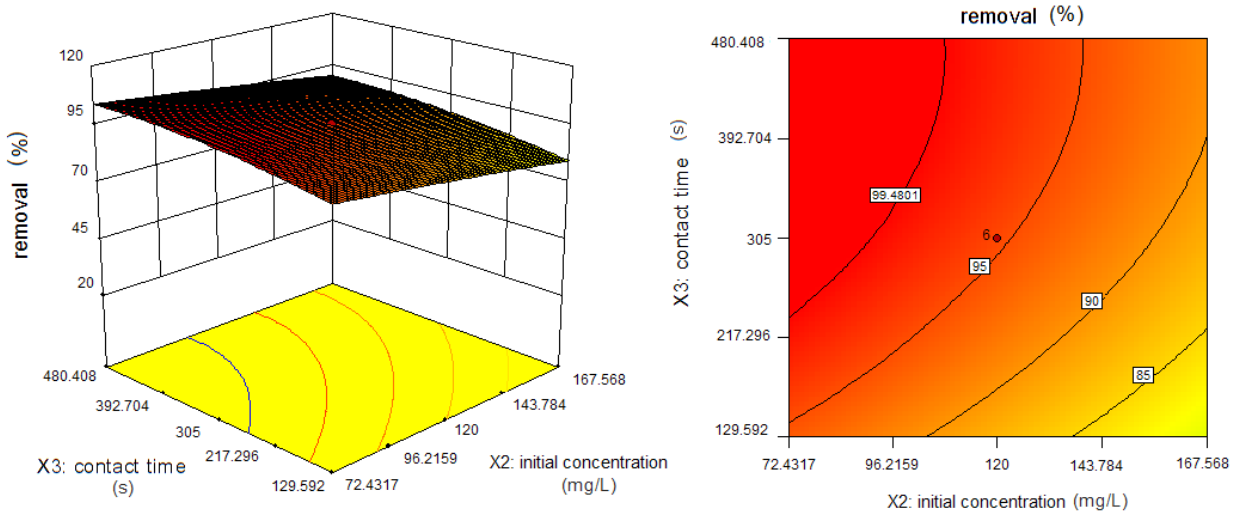

Fig. 3. The effect of initial MG concentration and contact time on the removal capacity, when the adsorbent dosage was fixed to 0.55 g/100 mL.

binder surfaces [27]. It is better to have a short contact time and low adsorbent dosage, when considered economically. Furthermore, Fig. 3 presents the effect of interaction between the initial concentration (X_2) and the contact time (X_3) on the removal efficiency, when adsorbent dosage is kept constant at 0.55 mg/100 mL. In addition to the findings that the effect of interaction between the initial MG concentration and the contact time is weak, as the contact time increased the removal efficiency increased and as the initial concentration increased the removal efficiency was reduced. In high concentration of MG, there are not enough spaces for dye due to lack of available active sites on the adsorbent surface [28].

Maximum removal efficiency with zeolite and suitable optimum experimental conditions of independent variables are determined using the desirability function of Design Expert Software (Fig. 4) [29]. The determined optimum
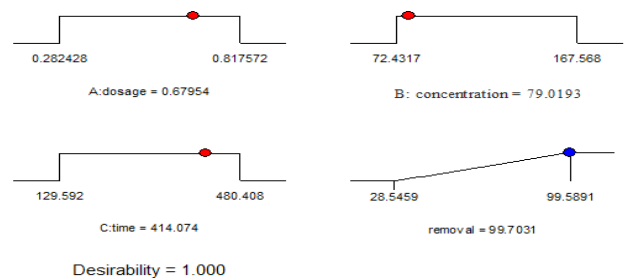

Fig. 4. Desirability ramp for numerical optimization of three independent variables, adsorbent dosage, initial MG concentration and contact time.

conditions are the adsorbent dosage of 0.68 mg/100 mL, the initial MG concentration of 79.02 mg/L and the contact time of 414 s. Under these conditions the removal efficiency is 99.70%.

3.2. Adsorption kinetics

In order to determine the adsorption mechanism kinetic models that include pseudo-first-order model [30], pseudo-second-order model [31] and intra-particle diffusion model [32] were implemented for this study.

The linear forms of pseudo-first-order model and pseudo-second-order model could be denoted with following equations, respectively:

$$\log(q_{eq} - q_{t)}) = \log q_{eq} - \frac{k_1 t}{2.203} \tag{5}$$

$$\frac{t}{q} = \frac{1}{k_2 q_{eq}^2} + \frac{1}{q_{eq}} t \tag{6}$$

where q_{eq} is the maximum adsorption capacity (mg/g), q_t and q are the MG amount adsorbed on zeolite at a given time (mg/g), k_1 (1/h) and k_2 (g/mg min) are the rate constants for pseudo-first-order and pseudo-second-order kinetic models, respectively.

Adsorption is a multi-step process that includes the transfer of dissolved molecules to the surface of the solid particles of the adsorbent from liquid phase and in a well-mixed batch adsorption system there is a probability of intra-particle diffusion for the adsorbate, which is a rate delimiter step. Therefore, it is necessary to determine the diffusion rate, since the diffusion of the dissolved molecules is conceivably a slow process [33]. Intra-particle diffusion parameter, K, could be found with the following equation:

$$q_t = Kt^{0.5} \tag{7}$$

where K is the intra-particle diffusion rate (mg/g min$^{-0.5}$). K value could be calculated from the slope of the curve of q_t vs. t.

The k_1, k_2, q_{eq} values and correlation coefficients for the pseudo-first-order and pseudo-second-order kinetic models that are obtained with different concentrations and the K constant of the intra-particle diffusion model are compared in Table 4. As indicated in Table 4, although correlation coefficients for both models are high and the correlation coefficients for the pseudo-second-order kinetic model were

found to be higher. Concurrently, theoretical q_{eq} values and experimental q_{eq} values yielded better with the pseudo-second-order kinetic model. K values increased with respect to the elevated MG concentration. This linear relationship indicates the high contribution of intra-particle diffusion on the adsorption process [34,35]. Kinetic results showed that the sorption process could be defined via pseudo-second-order kinetic model along with intra-diffusion, which is one of the rate determination steps.

3.3. Equilibrium isotherms

Langmuir and Freundlich isotherm models provide information on the trend of the adsorbent and characteristics of the mechanism for target types, through the analysis of the experimental equilibrium data [36]. Langmuir adsorption isotherm assumes a homogeneous surface energy distribution [37]. The linear form for Langmuir isotherm is represented as [38]:

$$q_{eq} = \frac{q_{max} b C_{eq}}{1 + b C_{eq}} \tag{8}$$

where q_{eq} is the MG amount adsorbed at the time of equilibrium (mg/g), C_{eq} is the equilibrium concentration of MG in the solution (mg/L), q_{max} is the maximum adsorption capacity (mg/g) and b is the adsorption equilibrium constant related to adsorption energy (L/mg).

The fundamental characteristics of Langmuir isotherm could be stated according to the dimensionless separation factor, R_L, and could be defined with the following expression [39]:

$$R_L = \frac{1}{1 + b C_0} \tag{9}$$

where C_0 is the initial MG concentration in the solution (mg/L).

Freundlich isotherm is used for liquid phase adsorption on a surface with heterogeneous energy distribution. This isotherm is represented with the following formula [40,41]:

$$q_{eq} = K_f C_{eq}^{1/n} \tag{10}$$

where K_f is an empirical constant to indicate the adsorption capacity, $1/n$ is the heterogeneity factor used to characterize the heterogeneity of the system.

Table 4
Kinetic parameters for the adsorption of MG with zeolite

C_o mg/L	$q_{eq,}$ mg/g	Pseudo first-order- kinetic			Pseudo second-order-kinetic			Intra-particle diffusion	
		k_1 1/min	$q_{eq,cal}$ mg/g	R^2	k_2 1/min	$q_{eq,cal}$ mg/g	R^2	K mg/(g min$^{-0.5}$)	R^2
40	7.78	0.332	1.25	0.901	3.192	7.81	0.999	0.0006	0.999
80	16.20	0.502	2.33	0.965	1.044	16.34	0.999	0.0383	0.912
120	22.08	0.355	7.78	0.891	0.191	23.04	0.999	0.0435	0.972
160	32.40	0.267	12.31	0.903	0.076	32.78	0.999	0.1142	0.950

Table 5
Isotherm coefficients for MG adsorbed on zeolite

Langmuir parameters		Freundlich parameters	
q_{max} (mg/g)	98.04	K_f (mg/g)	4.24
b (L/mg)	0.06	$1/n$	0.78
R^2	0.996	R^2	0.955

Table 6
Maximum adsorption capacities of MG from aqueous solution using various sorbents

Sorbents	q_{max} (mg/g)	References
Modified clay	40.48	[5]
China natural zeolite	27.34	[18]
Walnut shell	90.80	[35]
Modified breadnut peel	177.40	[44]
Carrot stem powder	55.50	[46]
Magnetic litchi pericarps	70.42	[47]
Modified hydroxyapatite	188.18	[48]
Avena sativa (oat) hull	83.00	[49]
Superparamagnetic sodium alginate-coated Fe_3O_4 nanoparticles	47.84	[50]
Carboxylate functionalized multi-walled carbon nanotubes	49.45	[51]
Used black tea	110.00	[52]
Chitin	97.09	[53]
Zeolite	98.04	This study

Table 5 presents the adsorption model constant values for the Langmuir and Freundlich isotherms. q_{max}, which denotes the maximum capacity, demonstrates total capacity of adsorbent or the single-layered saturation at equilibrium for MG. In Table 6, q_{max} value found in this study is compared to different adsorbents reported for MG removal. If $R_L > 1$, it is inconvenient; if $R_L = 1$, it is linear; $0 < R_L < 1$ is appropriate; and $R_L = 0$ is irreversible [39,40]. Retrieved R_L values are between 0.09 and 0.29. This result demonstrates that for removal of MG from aqueous solutions, zeolite, a natural adsorbent, is available for the adsorption process.

The Freundlich constant $(1/n)$ is related to the density of the sorbent. Adsorption is flawless when it is $0.1 < 1/n < 0.5$; adsorption is easy when $0.5 < 1/n < 0.1$; and adsorption is hard when $1/n > 1$ [42]. In this study, $1/n$ value found as 0.77 demonstrates that MG could easily be adsorbed on zeolite. Adsorption data is found to be more in accordance with the Langmuir model rather than the Freundlich model, when the correlation coefficients of the two isotherm models are compared.

3.4. Regeneration studies

Regeneration and subsequent reuse of the adsorbent are critical for industrial applications due to reduction of costs, continuous dependence of the adsorbent treatment process and possible recovery of the dye molecules [43]. Therefore, zeolite regeneration and reuse study was carried out in five cycles. In Fig. 5, removal efficiencies of zeolites (either using
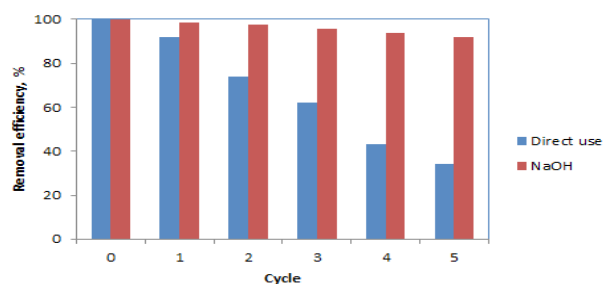

Fig. 5. Effect of regeneration and reuse on MG removal efficiency (adsorbent dosage: 0.68 mg/100 mL; initial MG concentration: 79.02 mg/L; contact time: 414 s).

directly without desorption or using after treatment with 0.1 M NaOH) used again in the adsorption of MG was compared. While at the end of the fifth cycle, MG removal efficiency of zeolite used directly declines to 30%, MG removal efficiency rate of the zeolite treated with NaOH and used again after the end of each cycle is still high (92%). Therefore, zeolite has great potential to be used in real-life application in wastewater treatment of MG dye since it can be reused by recycling the adsorbent and coupled with its ability at maintaining high removal efficiency after several cycles [44].

3.5. Characterization of adsorbent

In order to examine the morphology of zeolite and zeolite loaded MG, SEM is equipped with an energy dispersive X-ray detector. SEM images in Figs. 6(a) and (b) show coverage of the surface of the MG adsorbent due to adsorption of the adsorbate molecules presumably leading to formation of a monolayer of the adsorbate molecule over the adsorbent surface which is evident from the formation of white layer (molecular cloud) of uniform thickness and coverage (spread) [45]. The results of chemical analysis of the zeolite and MG loaded zeolite were obtained using semiquantitative EDX data, presented in Figs. 6(c) and (d), respectively (Idle picks are the gold palladium peaks caused by the coating). By the way of loading with MG, carbon content of zeolite sample was increased from 0.13% to 12.43%. This result which confirms the successful loading of MG is compatible with previous findings.

The FTIR spectrum of zeolite and zeolite loaded MG is presented in Fig. 7. For bulk zeolite, picks at 3,416 cm⁻¹ attributed to the stretching vibration of O–H; at 1,630 cm⁻¹ attributed to the stretching vibration of Al-OH group; at 1,019 cm⁻¹ attributed to asymmetric stretching vibration of either Si–O–Si or (Al–O–Al); at 791 cm⁻¹ attributed to symmetric Si–O–Si or Al–O–Al showing the in-plane bending. Picks formed after MG adsorption at 1,685 cm⁻¹ attributed to the stretching vibration of C=N, at 1,585 cm⁻¹ attributed to the stretching of aromatic C=C bond and at 1,370 cm⁻¹ attributed to the stretching vibration of $CH_3 – N$ bond. Comparing the two IR spectra; vibration peaks at 1,630 cm⁻¹ wavelength existing before adsorption, disappear with reacting with some existing groups in MG, parallel to the adsorption mechanism and characteristic picks belonging to MG at 1,685, 1,585 and 1,370 cm⁻¹ appeared. Therefore, it is logical to assume that MG adsorbed on zeolite.
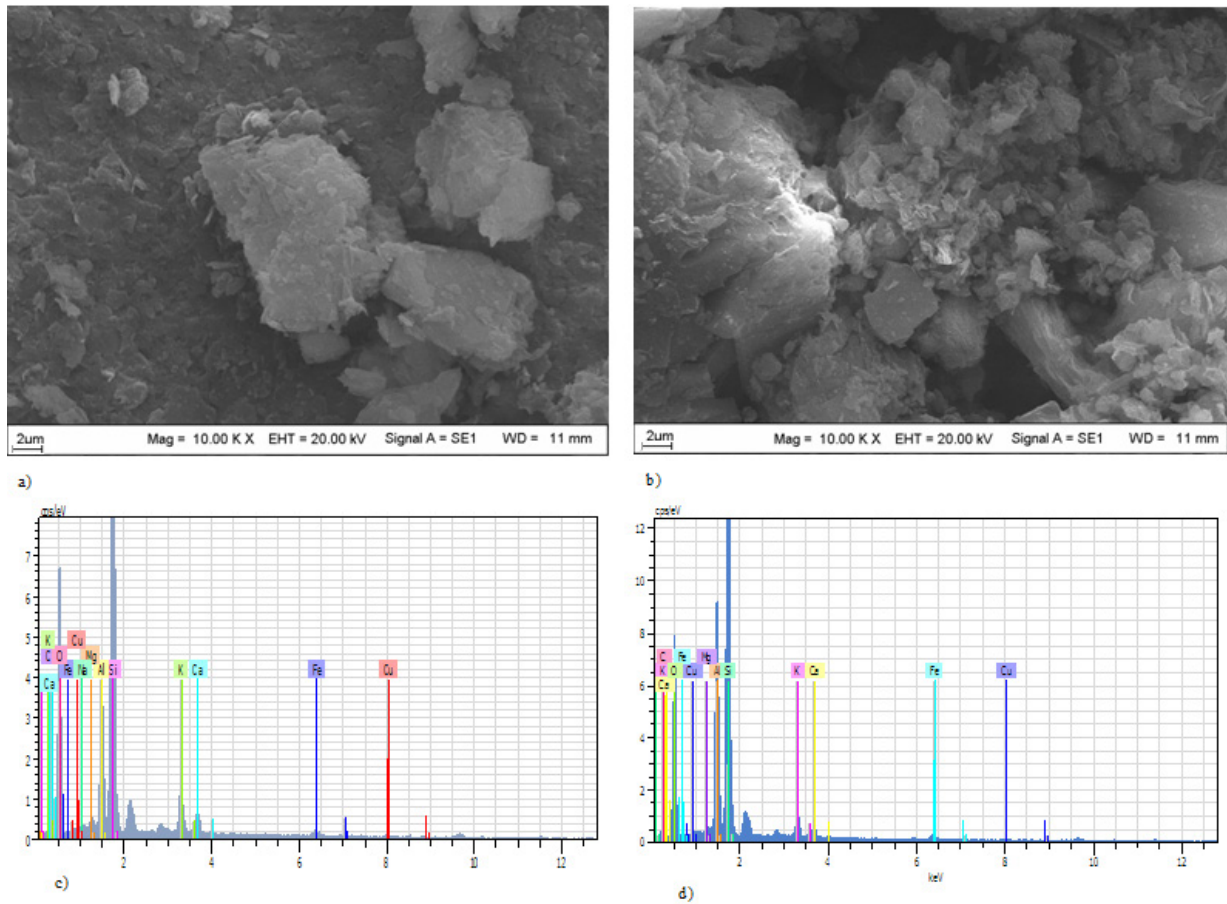
Fig. 6. SEM images of (a) zeolite; (b) zeolite after adsorption; (c) EDX analysis of zeolite; (d) EDX analysis of zeolite after adsorption.
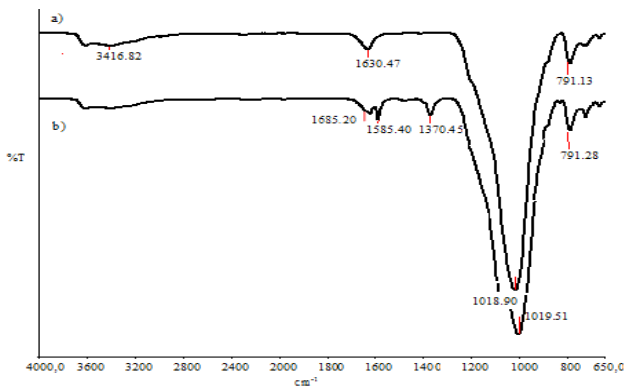

Fig. 7. FTIR spectra of (a) zeolite and (b) zeolite after adsorption.

4. Conclusions

In this study, CCD was used for compliance of experimental conditions for removal of MG by zeolite. The results pointed out that, when the adsorbent dosage, initial MG concentration and contact time are fixed to 0.68 mg/100 mL, 79.02 mg/g and 414 s, respectively, 99.70% maximum removal efficiency for MG is obtained. Quadratic model analysis proved sufficient sensitivity and confidence ($R^2 = 0.95$) of adsorption experiments of the model, for MG adsorption by zeolite. Adsorption isotherms provided good compliance with Langmuir model. Maximum adsorption capacity q_{max} is determined as 98.04 mg/g. Kinetics study was conducted based on pseudo-first-order, pseudo-second-order and intra-particle diffusion models. Adsorption kinetics could be explained by pseudo-second-order model in addition to the intra-particle diffusion model. Zeolite, used in this study, could be preferable in MG removal due to being subject to no type of modification process, being economical, being fast and efficient in MG adsorption.

Symbols

ANOVA — Analysis of variance
b — Langmuir constant for intensity of adsorption, L/mg
b_0 — Model constant
b_i — Linear coefficient

b_{ii}	—	Quadratic coefficient
b_{ij}	—	Cross-product coefficient
C_{eq}	—	Equilibrium concentration of malachite green in solution, mg/L
C_0	—	Initial malachite green concentration, mg/L
C_t	—	Malachite green concentration at time t, mg/L
CCD	—	Central composite design
EDX	—	Energy dispersive X-ray
DF	—	Degree of freedom
F	—	Fischer statistics
FTIR	—	Fourier transform infrared spectrometer
K	—	Intra-particle diffusion rate, mg/g min$^{-0.5}$
K_f	—	Freundlich constant of adsorption capacity
k_1	—	Rate constant for pseudo-first-order, 1/h
k_2	—	Rate constant for pseudo-second-order, g/mg/min
MG	—	Malachite green
Prob > F	—	Proportion of time or probability expected to obtain the stated F-value
q	—	Adsorbed malachite green amount, mg/g
q_{eq}	—	Malachite green amount adsorbed at equilibrium, mg/g
q_{max}	—	Maximum adsorption capacity, mg/g
q_t	—	Malachite green amount adsorbed at a time t, mg/g
R^2	—	Correlation coefficient
R_L	—	Langmuir constant of separation
RSM	—	Response surface methodology
SEM	—	Scanning electron microscopy
V	—	Volume of the solution, L
x_i and x_j	—	Independent variables
X_1	—	First factor, adsorbent dosage, mg/g
X_2	—	Second factor, initial malachite green concentration, mg/L
X_3	—	Third factor, contact time, s
y	—	Assumed response
1/n	—	Heterogeneity factor of Freundlich isotherm

Greek symbol

$\pm\alpha$	—	Axial points

References

[1] G.S. Dawood, Removal orange (G) dye from aqueous solution by adsorption on bentonite, Tikrit J. Pure Sci., 15 (2010) 231–234.

[2] F. Hemmati, R. Norouzbeigi, F. Sarbisheh, H. Shayesteh, Malachite green removal using modified sphagnum peat moss as a low-cost biosorbent: kinetic, equilibrium and thermodynamic studies, J. Taiwan Inst. Chem. E, 58 (2016) 482–489.

[3] Z. Lin, H. Zhang, A. Peng, Y. Lin, L. Li, Z. Huang, Determination of malachite green in aquatic products based on magnetic molecularly imprinted polymers, Food Chem., 200 (2016) 32–37.

[4] R. Ahmad, R. Kumar, Adsorption studies of hazardous malachite green onto treated ginger waste, J. Environ. Manage., 91 (2010) 1032–1038.

[5] S. Arellano-Cárdenas, S. López-Cortez, M. Cornejo-Mazón, J.C. Mares-Gutiérrez, Study of malachite green adsorption by organically modified clay using a batch method, Appl. Surf. Sci., 280 (2013) 74–78.

[6] M. Dastkhoon, M. Ghaedi, A. Asfaram, A. Goudarzi, S.M. Langroodi, I. Tyagi, S. Agarwal, V.K. Gupta, Ultrasound assisted adsorption of malachite green dye onto ZnS:Cu-NPAC: equilibrium isotherms and kinetic studies – Response surface optimization, Sep. Purif. Technol., 156 (2015) 780–788.

[7] K.Y.A. Lin, H.A. Chang, Ultra-high adsorption capacity of zeolitic imidazole framework-67 (ZIF-67) for removal of malachite green from water, Chemosphere, 139 (2015) 624–631.

[8] A. Singh, S.R. Manju, N.R. Bishnoi, Malachite green dye decolorization on immobilized dead yeast cells employing sequential design of experiments, Ecol. Eng., 47 (2012) 291–296.

[9] Y. Yang, H. Hu, G. Wang, Z. Li, B. Wang, X. Jia, Y. Zhao, Removal of malachite green from aqueous solution by immobilized *Pseudomonas* sp. DY1 with *Aspergillus oryzae*, Int. Biodeter. Biodegr., 65 (2011) 429–434.

[10] S. Çoruh, S. Elevli, Optimization of malachite green dye removal by sepiolite clay using a central composite design, Global NEST J., 16 (2014) 340–348.

[11] J. Zhang, Y. Li, C. Zhang, Y. Jing, Adsorption of malachite green from aqueous solution onto carbon prepared from *Arundo donax* root, J. Hazard. Mater., 150 (2008) 774–782.

[12] I.A. Rahman, B. Saad, S. Shaidan, E.S. Sya Rizal, Adsorption characteristics of malachite green on activated carbon derived from rice husks produced by chemical–thermal process, Bioresour. Technol., 96 (2005) 1578–1583.

[13] V.K. Garg, R. Kumar, R. Gupta, Removal of malachite green dye from aqueous solution by adsorption using agro-industry waste: a case study of *Prosopis cineraria*, Dyes Pigments, 62 (2004) 1–10.

[14] C.P. Sekhar, S. Kalidhasan, V. Rajesh, N. Rajesh, Bio-polymer adsorbent for the removal of malachite green from aqueous solution, Chemosphere, 77 (2009) 842–847.

[15] G. Kiani, M. Dostali, A. Rostami, A.R. Khataee, Adsorption studies on the removal of malachite green from aqueous solutions onto halloysite nanotubes, Appl. Clay Sci., 54 (2011) 34–39.

[16] M. Shirmardi, A.H. Mahvi, A.N. Bayram, G. Hashemzadeh Hassani, M.V. Niri, The adsorption of malachite green (MG) as a cationic dye onto functionalized multi walled carbon nanotubes, Korean J. Chem. Eng., 30 (2013) 1603–1608.

[17] C.H. Weng, Y.F. Pan, Adsorption of a cationic dye (methylene blue) onto spent activated clay, J. Hazard. Mater., 144 (2007) 355–362.

[18] R. Han, Y. Wang, Q. Sun, L. Wang, J. Song, X. He, C. Dou, Malachite green adsorption onto natural zeolite and reuse by microwave irradiation, J. Hazard. Mater., 175 (2010) 1056–1061.

[19] G.H. Mirzabe, A.R. Keshtkar, Application of response surface methodology for thorium adsorption on PVA/Fe$_3$O$_4$/SiO$_2$/APTES nanohybrid adsorbent, J. Ind. Eng. Chem., 26 (2015) 277–285.

[20] A. Azizi, M.R. Alavi Moghaddam, M. Arami, Application of wood waste for removal of reactive blue 19 from aqueous solutions: optimization through response surface methodology, Environ. Eng. Manage. J., 1 (2012) 795–804.

[21] V. Yönten, N. Aktaş, Exploring the optimum conditions for maximizing the microbial growth of Candida Intermedia by response surface methodology, Prep. Biochem. Biotechnol., 44 (2014) 26–39.

[22] R. Kumar, R. Singh, N. Kumar, K. Bishnoi, N. Bishnoi, Response surface methodology approach for optimization of biosorption process for removal of Cr (VI), Ni (II) and Zn (II) ions by immobilized bacterial biomass sp. *Bacillus brevis*, Chem. Eng. J., 146 (2009) 401–407.

[23] V. Yonten, Detecting optimum and cost-efficient of microbial growth rate and lactose consumption of Kluyveromyces lactis Y-8279 using RSM, Digest J. Nanomater. Biostruct., 8 (2013) 1283–1295.

[24] O. Tepe, Y.A. Dursun, Exo-pectinase production by *Bacillus pumilus* using different agricultural wastes and optimizing of medium components using response surface methodology, Environ. Sci. Pollut. R, 21 (2014) 9911–9920.

[25] W.T. Tsai, K.J. Hsien, H.C. Hsu, C.M. Lin, K.Y. Lin, C.H. Chiu, Utilization of ground eggshell waste as an adsorbent for the removal of dyes from aqueous solution, Bioresour. Technol., 99 (2008) 1623–1629.

[26] P.F. Sales, Z.M. Magriotis, M.A.L.S. Rossi, R.F. Resende, C.A. Nunes, Comparative analysis of tropaeolin adsorption onto raw and acid-treated kaolinite: optimization by response surface methodology, J. Environ. Manage., 151 (2015) 144–152.

[27] A. Saeed, M.W. Akhtar, M. Iqbal, Removal and recovery of heavy metals from aqueous solution using papaya wood as a new biosorbent, Sep. Purif. Technol., 45 (2005) 25–31.

[28] K. Kalantari, M.B. Ahmad, H.R.F. Masoumi, K. Shameli, M. Basri, R. Khandanlou, Rapid and high capacity adsorption of heavy metals by Fe_3O_4/montmorillonite nanocomposite using response surface methodology: preparation, characterization, optimization, equilibrium isotherms, and adsorption kinetics study, J. Taiwan Ins. Chem. Eng., 49 (2015) 192–198.

[29] M. Roosta, M. Ghaedi, A. Daneshfar, R. Sahraei, A. Asghari, Optimization of the ultrasonic assisted removal of methylene blue by gold nanoparticles loaded on activated carbon using experimental design methodology, Ultrason. Sonochem., 21 (2014) 242–252.

[30] S.V. Mohan, N.C. Rao, K.K. Prasad, J. Karthikeyan, Treatment of simulated Reactive Yellow 22 (Azo) dye effluents using Spirogyra species, Waste Manage., 22 (2002) 575–582.

[31] Y.S. Ho, G. McKay, Sorption of dye from aqueous solution by peat, Chem. Eng. J., 70 (1998) 115–124.

[32] J. Fu, Z. Chen, M. Wang, S. Liu, J. Zhang, J. Zhang, R. Han, Q. Xu, Adsorption of methylene blue by a high-efficiency adsorbent (polydopamine microspheres): kinetics, isotherm, thermodynamics and mechanism analysis, Chem. Eng. J., 259 (2015) 53–61.

[33] H. Tang, W. Zhou, L. Zhang, Adsorption isotherms and kinetics studies of malachite green on chitin hydrogels, J. Hazard. Mater., 209–210 (2012) 218–225.

[34] B.H. Hameed, Equilibrium and kinetic studies of methyl violet sorption by agricultural waste, J. Hazard. Mater., 154 (2008) 204–212.

[35] M.K. Dahri, M.R.R. Kooh, L.B.L. Lim, Water remediation using low cost adsorbent walnut shell for removal of malachite green: equilibrium, kinetics, thermodynamic and regeneration studies, J. Environ. Chem. Eng., 2 (2014) 1434–1444.

[36] U. Guyo, T. Makawa, M. Moyo, T. Nharingo, B.C. Nyamunda, T. Mugadza, Application of response surface methodology for Cd(II) adsorption on maize tassel-magnetite nanohybrid adsorbent, J. Environ. Chem. Eng., 3 (2015) 2472–2483.

[37] B. Sarkar, R. Naidu, M. Megharaj, Simultaneous adsorption of tri- and hexavalent chromium by organoclay mixtures, Water Air Soil Pollut., 224 (2013) 1–10.

[38] I. Langmuir, The adsorption of gases on plane surfaces of glass, mica and platinum, J. Am. Chem. Soc., 40 (1918) 1361–1403.

[39] Y. Xue, H. Hou, S. Zhu, Competitive adsorption of copper (II), cadmium (II), lead (II) and zinc (II) onto basic oxygen furnace slag, J. Hazard. Mater., 162 (2009) 391–401.

[40] M.A. Ahmad, R. Alrozi, Removal of malachite green dye from aqueous solution using rambutan peel-based activated carbon: equilibrium, kinetic and thermodynamic studies, Chem. Eng. J., 171 (2011) 10–516.

[41] H.M.F. Freundlich, Over the adsorption in solution, J. Phys. Chem., 57 (1906) 385–470.

[42] B. Samiey, M. Dargahi, Kinetics and thermodynamics of adsorption of congo red on cellulose, Cent. Eur. J. Chem., 8 (2010) 906–912.

[43] D. Charumathi, N. Das, Packed bed column studies for the removal of synthetic dyes from textile wastewater using immobilized dead *C. tropicalis*, Desalination, 285 (2012) 22–30.

[44] H.I. Chieng, L.B.L. Lim, N. Priyantha, Enhancing adsorption capacity of toxic malachite green dye through chemically modified breadnut peel: equilibrium, thermodynamics, kinetics and regeneration studies, Environ. Technol., 36 (2015) 86–97.

[45] C. Namasivayam, D. Kavitha, IR, XRD and SEM studies on the mechanism of adsorption of dyes and phenols by coir pith carbon from aqueous phase, Microchem. J., 82 (2006) 43–48.

[46] A.K. Kushwaha, N. Gupta, M.C. Chattopadhyaya, Removal of cationic methylene blue and malachite green dyes from aqueous solution by waste materials of *Daucus carota*, J. Saudi Chem. Soc., 18 (2014) 200–207.

[47] H. Zheng, J. Qi, R. Jiang, Y. Gao, X. Li, Adsorption of malachite green by magnetic litchi pericarps: a response surface methodology investigation, J. Environ. Manage., 162 (2015) 232–239.

[48] A.A. El-Zahhara, N.S. Awwad, Removal of malachite green dye from aqueous solutions using organically modified hydroxyapatite, J. Environ. Chem. Eng., 4 (2016) 633–638.

[49] S. Banerjee, G.C. Sharma, R.K. Gautam, M.C. Chattopadhyaya, S.N. Upadhyay, Y.C. Sharma, Removal of malachite green, a hazardous dye from aqueous solutions using Avena sativa (oat) hull as a potential adsorbent, J. Mol. Liq., 213 (2016) 162–172.

[50] A. Mohammadi, H. Daemi, M. Barikani, Fast removal of malachite green dye using novel superparamagnetic sodium alginate-coated Fe_3O_4 nanoparticles, Int. J. Biol. Macromol., 69 (2014) 447–455.

[51] H. Sadegh, R. Shahryari-ghoshekandi, S. Agarwal, I. Tyagi, M. Asif, V.K. Gupta, Microwave-assisted removal of malachite green by carboxylate functionalized multi-walled carbon nanotubes: kinetics and equilibrium study, J. Mol. Liq., 206 (2015) 151–158.

[52] M.A. Hossain, M.L. Hossain, M.T. Hassan, Equilibrium, thermodynamic and mechanism studies of malachite green adsorption on used black tea leaves from acidic solution, Int. Lett. Chem. Phys. Astron., 64 (2016) 77–88.

[53] M. Sriuttha, K. Wittayanarakul, Comparison of thermodynamics and kinetics of malachite green adsorption onto chitin and chitosan, Asian J. Chem., 27 (2015) 4213–4215.